Scientific Papers. Series E. Land Reclamation, Earth Observation & Surveying, Environmental Engineering. Vol. XV, 2026
Print ISSN 2285-6064, CD-ROM ISSN 2285-6072, Online ISSN 2393-5138, ISSN-L 2285-6064

INTERNAL AIR RECIRCULATION FOR CONDENSATION RISK CONTROL IN PASSIVE SOLAR GREENHOUSES: A DEW MARGIN-BASED ZONAL APPROACH

Bogdan ILIE[1], Yuxin TONG[2], Ana BUTCARU[1], Tiberiu ION[3], Ionuț Ovidiu JERCA[1]

[1]University of Agronomic Sciences and Veterinary Medicine of Bucharest,
59 Mărăști Blvd, District 1, Bucharest, Romania
[2]Institute of Environment and Sustainable Development in Agriculture,
Chinese Academy of Agricultural Sciences, China
[3]SC Skip Monday Studio SRL, 10 Triumfului Street, Ploiesti, Prahova County, Romania

Corresponding author email: ovidiu.jerca@qlab.usamv.ro

Abstract

During winter operation, passive solar greenhouses with limited auxiliary heating are frequently affected by nocturnal thermal stratification and elevated humidity, promoting condensation on structural surfaces and increasing fungal disease risk at canopy level. This study evaluates an internal air recirculation strategy for condensation prevention, implemented in a double-layer Chinese solar greenhouse at the University of Agronomic Sciences and Veterinary Medicine of Bucharest. Twenty axial fans were installed at 3.5 m height along both longitudinal sides, controlled by adaptive dew margin thresholds derived from a distributed canopy sensor network. Two experimental phases were compared: Phase I used synchronized control of both ventilation units driven by the worst-case canopy dew margin; Phase II introduced asynchronous zonal control, with each unit independently responding to its local canopy sensor. Results indicate that canopy-based recirculation control successfully maintained positive dew margins at plant level throughout the monitoring period, with no leaf wetness events detected at canopy level in either phase, while structural condensation on the inner polyethylene cover persisted. The dew margin indicator proved more operationally discriminating than relative humidity alone under the conditions observed.

Key words: *condensation risk, dew point, internal recirculation, passive greenhouse, zonal microclimate control.*

INTRODUCTION

Winter greenhouse operation in passive or semi-closed structures is frequently constrained by limited external ventilation, either due to energy penalties or the risk of cold stress for sensitive crops. Under such conditions, relative humidity often remains high, and localized stagnant air zones may develop, promoting condensation on cold structural surfaces and, in some cases, within the crop canopy. Condensation is not only an undesirable physical phenomenon but also a major biological risk factor, strongly associated with fungal disease development and reduced crop quality during the cold season (Piscia et al., 2012; Amani et al., 2020). This challenge becomes particularly acute in greenhouses with modest auxiliary heating, where nocturnal thermal stratification leads to the accumulation of warm, humid air in the upper volume while the crop zone remains prone to saturated boundary layers.

From a physical perspective, condensation is governed by the proximity of air temperature to the dew point and the presence of sufficiently cold surfaces acting as sinks for water vapor. In greenhouse environments, nocturnal radiative cooling of the envelope is often the dominant driver, making the roof or inner cover the coldest surface where condensation is initiated (Piscia et al., 2012). Consequently, dew point-based indicators provide a more robust framework for condensation risk assessment than relative humidity alone, since they quantify the thermodynamic margin to saturation. Moreover, condensation typically develops locally in the coldest or most humid zones, meaning that bulk-average climate variables may fail to capture critical risk conditions (Boulard & Draoui, 1995; Gao et al., 2024).

Natural ventilation remains the classical tool for controlling temperature and humidity, yet its effectiveness depends strongly on wind conditions, buoyancy forces, vent geometry, and

the effective opening area. Experimental studies and models have shown that ventilation rates generally increase with wind speed and vent aperture, but the relationship is highly variable and sensitive to airflow regimes and structural design (Boulard & Draoui, 1995; Baptista et al., 1999; Teitel & Tanny, 1999). Because ventilation rate fluctuates continuously with weather conditions, its reliable characterization requires real-time measurement rather than static assumptions (Tusi & Shimazu, 2020). Importantly, seemingly secondary parameters such as pressure and discharge coefficients can substantially affect ventilation predictions; wind tunnel measurements have demonstrated clear dependencies on wind direction and vent configuration (Sase et al., 1980). Therefore, during winter, when vent opening is deliberately restricted, external ventilation becomes both difficult and energetically costly as a dehumidification strategy. In addition to energy limitations, modern greenhouses frequently employ insect-proof screens, which can significantly reduce effective ventilation due to increased aerodynamic resistance, thereby enhancing humidity accumulation and microclimate heterogeneity (Katsoulas et al., 2006). Under cold-season conditions, this creates a critical trade-off: ventilation sufficient to remove moisture may induce excessive heat losses and compromise energy efficiency. Studies quantifying the thermal cost of dehumidification have shown that a substantial fraction of heating energy may be indirectly expended through moisture removal via ventilation, motivating alternative or complementary approaches with reduced losses (Maslak & Nimmermark, 2017; Amani et al., 2020). Mechanical humidity-control options have been proposed for winter operation, yet their effectiveness must be evaluated in relation to thermal impacts and crop-zone relevance (Lee et al., 2020).

A key point emphasized in recent literature is that "ventilation" does not simply refer to air exchange rates, but rather to internal airflow patterns and climate uniformity at canopy level. Spatial heterogeneity in temperature and humidity may persist even in ventilated greenhouses, and stagnant zones can remain critical hotspots for condensation risk (Gao et al., 2024). This is consistent with experimental and CFD-based studies showing that ventilation design strongly determines distributed microclimate rather than only mean conditions (Bournet & Boulard, 2010; Zhang et al., 2025). Seasonal differences are also important: while summer ventilation is dominated by cooling requirements, winter ventilation must address humidity control under strong energy constraints (Kittas et al., 2005; He et al., 2015). Classical work has highlighted that air movement and climate uniformity are central objectives in greenhouse operation, not merely side-effects of vent opening (Sase, 2006).

Biologically, the relevant humidity is not necessarily the greenhouse-average value but the microclimate in the immediate vicinity of leaves, where boundary-layer effects may produce conditions substantially different from bulk air. Experimental evidence confirms that ventilation influences not only greenhouse humidity but also leaf boundary-layer humidity, with direct implications for condensation and disease risk (Boulard et al., 2004). Similarly, research on leaf wetness duration indicates that simple empirical thresholds (e.g., RH > 90%) may be insufficient in greenhouse environments, where spatial variability is high and locally calibrated models are required (Wang et al., 2019). These findings support approaches that explicitly separate structural condensation zones from agronomically relevant canopy zones and rely on physically grounded indicators such as dew point or dew margin combined with distributed sensing.

Alongside external air exchange strategies, increasing attention has been directed toward internal air recirculation and mixing as means to reduce stratification and limit the persistence of humid stagnant pockets without major ventilation heat losses. Horizontal airflow fan systems have been discussed as practical tools for reducing vertical gradients, improving canopy drying, and lowering the probability of reaching dew point at leaf level (Blanchard, 2008). Recent studies further indicate that non-uniform ventilation and airflow distribution can affect both energy consumption and plant growth, reinforcing the need for canopy-oriented microclimate control rather than reliance on bulk averages (Wang et al., 2025). CFD simulations of greenhouse airflow similarly emphasize the sensitivity of internal climate to geometry and vent configuration, making uniformity a design target rather than an automatic outcome (Zhang et al., 2025).

Based on these converging gaps in the literature, a clear applied problem emerges in passive winter greenhouses where external ventilation is restricted, there is a need for condensation-risk mitigation strategies that do not depend primarily on-air exchange with the outdoor environment. The present study therefore evaluates an internal air recirculation approach implemented in a double-layer passive greenhouse, using multi-point monitoring and dew point-based control indicators. Rather than treating the greenhouse climate as a single average value, the approach emphasizes (i) spatial characterization of microclimate variability, (ii) conservative worst-case risk definition, and (iii) canopy-oriented zonal control to limit stratification and condensation-prone stagnation zones. We hypothesized that independent control of lateral compartments, driven by local canopy dew margin measurements, would enhance protection against canopy-level condensation - thereby reducing the risk of fungal disease development - compared to a synchronized worst-case control strategy.

MATERIALS AND METHODS

Greenhouse structure and winter experimental context

The experiment was conducted during the cold season (December 2025 - February 2026) in a passive double-layer Chinese solar greenhouse located at the University of Agronomic Sciences and Veterinary Medicine of Bucharest, Romania. The structure analyzed in this study is referred to as the Solar Double Chinese greenhouse (SDC) and is used for overwintering exotic and subtropical crops under minimal conventional heating input (Figure 1).



Figure 1. Overview of the passive double-layer Chinese solar greenhouse used in the experiment (December 2025 – February 2026). Left: eastern compartment showing blueberry crops. Right: western compartment with tropical species, illustrating the spatial heterogeneity of the experimental environment.

The greenhouse has an external length of approximately 45 m and an internal length of 42 m, due to the presence of two independent polyethylene layers (outer and inner envelope). The usable internal width is approximately 18 m (20 m external), while the maximum internal height reaches about 6 m, a geometry that strongly promotes nocturnal thermal stratification during winter conditions.

Such stratification is a well-known feature of passive greenhouses operating under limited ventilation, where warm humid air accumulates in the upper volume while the crop zone remains prone to saturation (Sase, 2006; Piscia et al., 2012). The structure is oriented along the South-North axis and is longitudinally divided by a central corridor approximately 2 m wide, separating two main compartments referred to in this study as the eastern zone and the western zone.

Heating system and nocturnal stratification

Auxiliary heating is provided by 18 radiant electric panels installed above the central corridor at a height of approximately 2.5 m. Each panel has a nominal power of 500 W, resulting in a total installed capacity of approximately 9 kW. Under typical winter

operation, this radiant system generates a warm and humid air reservoir accumulating in the upper greenhouse volume. In the absence of sufficient circulation, the crop zone remains prone to stagnant moisture-laden boundary layers. Relative humidity frequently exceeds 90%, and condensation develops preferentially on cold structural surfaces (polyethylene foil and metallic elements), increasing the risk of fungal diseases and latent heat losses. Nocturnal radiative cooling of the envelope has been identified as a dominant driver of condensation initiation in greenhouse environments (Piscia et al., 2012). Natural ventilation through lateral openings is strongly restricted during winter, since external air is often too cold for subtropical crops and would induce significant energy penalties. Therefore, this study focuses on condensation-risk mitigation without relying on external air exchange, using only internal air recirculation, consistent with the need for low-energy humidity control strategies in winter greenhouses (Maslak & Nimmermark, 2017; Amani et al., 2020).

Internal air recirculation system

To reduce thermal stratification and limit condensation-prone microclimates, an internal air recirculation system was installed, consisting of 20 axial fans, each rated at approximately 40 W with a nominal airflow of about 400 $m^3\ h^{-1}$. Fans were mounted longitudinally at approximately 3.5 m height, distributed symmetrically: 10 fans on the eastern side and 10 fans on the western side. Airflows are directed downward toward the crop zone, aiming to create a turbulent mixing loop: warm humid air accumulated above the radiant heaters is pushed downward, while cooler air near the polyethylene envelope is mixed upward along the structural surface. This strategy is intended to weaken stratification and reduce the persistence of saturated boundary layers, without the energy losses associated with external ventilation (Blanchard, 2008; Bournet & Boulard, 2010). Fans were physically installed in early December 2025, while automated operation was implemented beginning in January 2026 after full integration into the Home Assistant control platform.

Distributed microclimate monitoring network (Figure 2 and Figure 3).



Figure 2. Internal air recirculation system. Left: recirculation fans (10 per side) mounted at ~3.5 m height, directed downward toward the crop zone. Right: TROTEC BA06 vane anemometer used for air velocity measurement during fan characterization trials



Figure 3. Schematic cross-section of the greenhouse illustrating the nocturnal thermal stratification pattern generated by the central radiant heating corridor and the air recirculation loops induced by the axial fans mounted at 3.5 m height on each longitudinal side (left). The VENTS VKOM 200 axial fan unit (43 W, 405 $m^3 \cdot h^{-1}$, 1300 rpm, IP X4) used for internal air recirculation (right)

Distributed microclimate monitoring network

Microclimate monitoring was performed through a distributed sensor network measuring air temperature and relative humidity at multiple vertical and lateral positions, designed to capture spatial gradients associated with condensation development. Spatial heterogeneity is frequently observed even in ventilated greenhouses, and local stagnant zones may remain critical hotspots for condensation risk (Gao et al., 2024). The initial monitoring configuration included sensors positioned in peripheral regions influenced by envelope cooling: S4 (Eastern zone, 100 cm above ground), S6 (Western zone, 100 cm above ground), S5 (Central upper volume, 400 cm height), and S8 (Southern upper zone, 400 cm height).

These sensors enabled computation of spatial dew point distributions and identification of structural zones with elevated condensation risk. Although S4 and S6 are defined by their mounting height (100 cm), their relatively marginal placement means they primarily reflect structural condensation conditions rather than direct canopy microclimate. The upper central sensor (S5) was used to characterize the general moisture reservoir in the greenhouse air mass, whereas fan control was always driven by the minimum (worst-case) dew margin measured in the canopy zone (Figure 4).



Figure 4. Canopy-level sensor deployment. Left: Sensor S1 (East compartment, 170 cm height) labelled with identification tag. Right: Sensor S2 (West compartment, 170 cm height). Both sensors measure air temperature and relative humidity for dew point and dew margin computation

Leaf wetness sensor and foil-adjacent measurements

A leaf wetness sensor (LWS) was deployed as a qualitative indicator of liquid water film formation. The sensor was validated prior to deployment by direct application of a water film (spray and moist tissue contact), confirming that it responds exclusively to liquid water film formation and remains at zero output in the absence of free water. When positioned within the crop canopy, the sensor recorded zero output throughout the entire monitoring period. When attached directly to the inner polyethylene foil surface - where condensation was visually confirmed on multiple nights - the sensor consistently detected condensation events. Repositioning the sensor 5 cm away from the foil surface was sufficient to return output to zero, confirming that condensation was confined to the immediate foil surface and did not extend into the adjacent air volume or the crop zone. This distinction between structural condensation and biologically relevant canopy wetness is consistent with studies showing that leaf boundary-layer humidity may differ substantially from bulk greenhouse air conditions (Boulard et al., 2004). The absence of liquid water detection within the canopy should be interpreted as evidence that the recirculation strategy successfully prevented leaf-level condensation, while structural condensation remained confined to the inner envelope. Leaf wetness duration models often require calibration beyond simple RH thresholds, highlighting the complexity of canopy-level moisture processes (Wang et al., 2019).

Three auxiliary temperature probes (Temperature 1–Temperature 3) were installed near the inner foil surface at different heights (30 cm, 150 cm, and 300 cm). Initially fixed directly on the foil, these probes primarily reflected surface cooling. Beginning on 1 February 2026, they were repositioned approximately 5 cm away from the foil, in order to better capture air temperature variations influenced by recirculation rather than direct conductive coupling to the cold surface (Figure 5).



Figure 5. Foil-adjacent temperature probe installation (Mobile Sensor 10). Left: Temperature 1 probe positioned at foil surface level. Right: Temperature 2 probe mounted inside the foil layer. Both probes monitor the thermal regime near the inner cladding surface to detect condensation-prone zones

Dew point computation and dew margin indicator

To evaluate condensation risk physically, dew point temperature was calculated using the Magnus–Tetens approximation, based on measured air temperature and relative humidity:

$$T_{te}^{W} = b \cdot \gamma(T,RH) / [a - \gamma(T,RH)]$$
$$\gamma(T,RH) = \ln(RH/100) + aT / (b + T)$$

where T is the air temperature (°C), RH is the relative humidity (%), and γ(T, RH) is an intermediate dimensionless variable used in the Magnus-Tetens formulation. The constants were set to a = 17.27 and b = 237.7°C, which are commonly applied for temperature ranges relevant to greenhouse environments.

Condensation proximity was expressed through the thermodynamic indicator dew margin, defined as:

$$\Delta T = T_a^{IR} - T_{te}^{W}$$

Large values indicate air far from saturation, whereas small values indicate proximity to condensation. Dew point–based indicators provide a more robust condensation-risk framework than relative humidity alone, particularly under heterogeneous greenhouse conditions (Piscia et al., 2012). In this study, the primary operational threshold was set at 2°C, while values below 1°C were considered indicative of imminent condensation risk within the crop zone.

Definition of the critical scenario: Worst-Case Dew Margin

In large greenhouse volumes, condensation develops locally in the coldest or most humid regions rather than uniformly. For preventive control, a conservative indicator termed Worst-Case Dew Margin was defined as the minimum dew margin value across monitored points:

$$\Delta T_m^{In} = min(\Delta T_1, \Delta T_2, \ldots, \Delta T_n)$$

This parameter continuously represents the point closest to condensation and serves as the main control variable for fan automation, consistent with the need for worst-case microclimate assessment rather than bulk averages (Gao et al., 2024).

Transition to canopy-based control (1 February 2026)

During the initial phase (December 2025-January 2026), worst-case control was dominated by marginal sensors (S4/S6) influenced by envelope cooling. While this configuration reflected structural condensation risk on the foil, it did not directly demonstrate agronomically relevant improvement in the leaf-level microclimate. To ensure biological relevance, two additional sensors were installed in the canopy zone on 1 February 2026: S1 (East canopy, 170 cm) and S2 (West canopy, 170 cm). These sensors are positioned within the vegetative zone, approximately 3.5 m from the fans, providing representative measurements of leaf-level temperature and humidity. From this date onward, fan automation was based exclusively on the canopy worst-case dew margin, while marginal sensors remained monitored as structural reference. The importance of canopy-oriented microclimate monitoring has been emphasized in studies addressing boundary-layer humidity and crop-level risk processes (Boulard et al., 2004; Sase, 2006).

Experimental Phase I - Synchronized canopy-based control

Between 1 February 2026 and 11 February 2026 (09:59), the system operated under a synchronized canopy-based control configuration, hereafter referred to as Phase I. During this interval, both ventilation units (Vent1 - East and Vent2 - West) were driven simultaneously by the canopy worst-case dew margin (S1), defined as the minimum ΔT among canopy sensors. This configuration ensured a conservative, homogeneous response across the greenhouse volume, treating the structure as a single thermodynamic control domain. Phase I thus represents the baseline experimental configuration against which subsequent zonal refinements are evaluated.

Beginning on 1 February 2026, internal air recirculation was controlled through an adaptive three-regime strategy:

- Critical regime (ΔT < 1.0°C) - fans operate continuously, indicating maximum agronomic condensation risk in the canopy.
- Intermediate regime (1.0-2.0°C) - fans operate in pulse mode (10 min ON / 20 min OFF), maintaining mixing while reducing energy consumption.
- Safe regime (ΔT > 2.5°C) - fans are fully switched off after stabilization, introducing hysteresis and preventing excessive cycling.

A hysteresis margin was introduced to prevent rapid fan cycling: recirculation was activated when ΔT fell below 2.0°C but switched off only after recovery above 2.5°C. Adaptive strategies with hysteresis are consistent with recommendations to avoid excessive switching while maintaining canopy-level uniformity (Bournet & Boulard, 2010; Zhang et al., 2025).

Transition to Phase II – Asynchronous canopy-based zonal control

Beginning on 12 February 2026, the control strategy was experimentally modified in order to evaluate the effect of spatially differentiated canopy-based recirculation. While Phase I relied on a synchronised worst-case control approach, both ventilation units being driven by the minimum canopy dew margin (S1), Phase II introduces an asynchronous zonal configuration. In this second phase, Vent1 (East compartment) continues to be controlled by the canopy worst-case dew margin (S1), whereas Vent2 (West compartment) is independently driven by the local canopy dew margin measured at S2 (170 cm height).

This modification was motivated by the persistent lateral asymmetry observed during Phase I, where S1 systematically exhibited lower dew margin values than S2. In addition, the eastern compartment is subjected to slightly higher irrigation frequency due to crop distribution, which may locally increase air humidity and influence dew point dynamics. Consequently, treating both compartments as a single homogeneous control volume may mask relevant microclimatic variability. The asynchronous configuration maintains identical thermodynamic thresholds (continuous operation for $\Delta T < 1°C$, pulse regime for 1-2°C, and shutdown above 2.5°C), ensuring comparability between phases while allowing independent zonal response.

Air velocity measurements

To quantify airflow intensity, air velocity was measured using a vane anemometer (TROTEC BA06) over 30-minute intervals at two locations: at 1.5 m from the fan (maximum velocity ≈ 1.0 m s^{-1}) and at canopy level near S1, at 2.5 m distance (maximum velocity ≈ 0.4 m s^{-1}). Although measured canopy air velocities were moderate (~0.4 m s^{-1}), the primary objective was not intensive convective drying but the reduction of stratification and the homogenization of humidity distribution within the crop zone, consistent with the role of airflow uniformity emphasized by Sase (2006).

Operational condensation risk definition and intervention quantification

For automation and quantitative evaluation, a binary condensation risk sensor was defined as active when the canopy worst-case dew margin fell below the critical threshold of 2°C, indicating conditions favorable for condensation. To validate the system experimentally, not only fan triggering but also the duration of exposure and intervention were quantified through two cumulative history statistics sensors implemented in Home Assistant: Condensation Risk Time Today (total daily hours during which condensation risk was active) and Recirculation Runtime Today (total daily operating time of the internal recirculation system). These metrics provide a reproducible framework for comparing climatic pressure against the effective response of the control strategy.

Data acquisition and storage

All temperature, relative humidity, dew point, dew margin, and fan-state data were collected automatically through the Home Assistant platform and continuously stored in an InfluxDB time-series database. This infrastructure enables full reconstruction of temporal series and subsequent statistical analysis of microclimate evolution and system response under winter operating conditions (Figure 6).

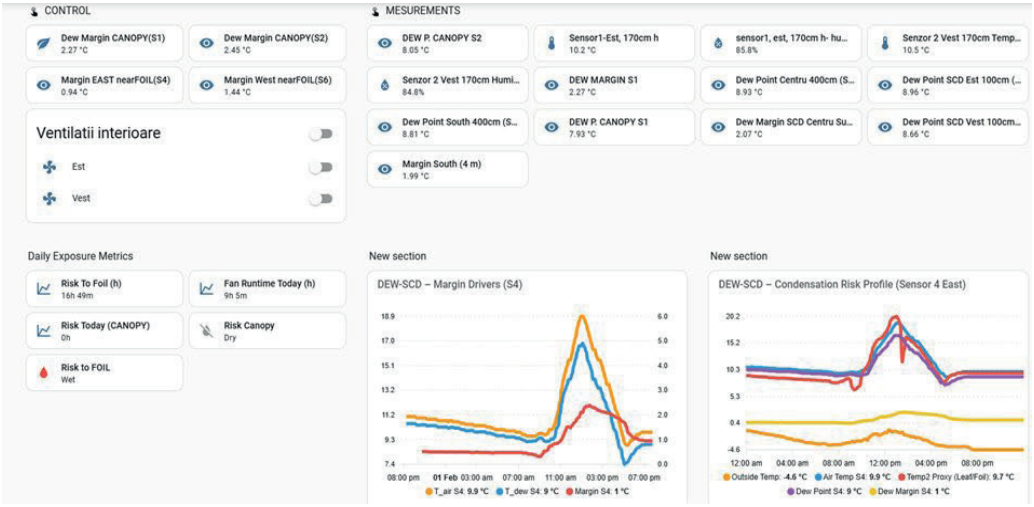


Figure 6. Home Assistant monitoring and control dashboard. Left panel: real-time dew margin values for all sensors and ventilator state. Centre: dew margin drivers time series (S4). Right: condensation risk profile for Sensor S4 (East). The dashboard integrates all sensor streams and provides visual indication of condensation risk zones

RESULTS AND DISCUSSIONS

Performance of the synchronised dew-margin-based recirculation control (Phase I)

During Phase I (1 February 2026 - 11 February 2026, 09:59), both recirculation fans (Vent1 - East compartment; Vent2 - West compartment) operated under a strictly synchronised control strategy, driven by the conservative canopy worst-case dew margin parameter (S1). Over the analysed interval of approximately 240 hours, both ventilation units exhibited nearly identical operational behaviour, with a cumulative runtime of 50.22 hours for Vent1 and 50.03 hours for Vent2, corresponding to an average daily operation of approximately 5 hours per ventilator. This confirms the deterministic and fully synchronised implementation of the initial control logic.

The distribution of canopy dew margin values during this phase indicates that the system maintained effective control over condensation risk. For the worst-case canopy parameter (S1), the cumulative duration during which the dew margin fell below 2°C was 164.56 hours, while the time spent below the more critical threshold of 1°C was limited to only 0.089 hours (approximately 5.3 minutes) over the entire observation period. The absolute minimum recorded value for S1 was 0.55°C, and the 5th percentile was 1.29°C, indicating that severe proximity to condensation conditions was rare and short-lived.

In contrast, the west-local canopy sensor (S2) exhibited less severe conditions. The cumulative time below 2°C was 139.11 hours, while no instances of dew margin below 1°C were recorded. The minimum observed value for S2 was 1.41°C, and the 5th percentile was 1.77°C. These results reveal a persistent lateral asymmetry between the two compartments, with the worst-case zone (S1) consistently exhibiting lower dew margin values and longer exposure to moderate condensation risk conditions compared to the western compartment.

Despite this spatial variability, both ventilation units operated with virtually identical runtimes due to the synchronised control strategy. Consequently, while the implemented logic proved effective in preventing severe condensation risk ($\Delta T < 1°C$) and maintained overall system stability, it did not account for lateral differences in microclimatic behaviour within the greenhouse. This observation provides the experimental justification for the subsequent implementation of an asynchronous, zone-based control strategy in Phase II.

Leaf wetness validation

The leaf wetness sensor, validated prior to deployment to confirm exclusive response to liquid water film, recorded zero output throughout the monitoring period when positioned within the canopy. This result is not attributable to sensor insensitivity: the same sensor consistently detected condensation events when in direct contact with the inner polyethylene foil surface, confirming both instrument functionality and the spatial confinement of condensation to structural surfaces. No leaf wetness events were recorded at canopy level during Phase I, despite multiple nocturnal intervals in which the dew margin approached critical thresholds. This indicates that the canopy-based control strategy successfully prevented actual condensation at plant level. Condensation was, however, visually observed on the greenhouse plastic cover during several nights, consistent with expected radiative cooling of structural surfaces. These observations confirm that dew margin values at canopy level remained above the condensation point even when structural surfaces experienced local cooling (Figure 7).



Figure 7. Home Assistant History record of canopy dew margin for S1 (East, blue) and S2 (West, yellow) during Phase I (1-11 February 2026), with ventilator activation states shown in the upper panel. Nocturnal peaks correspond to critical condensation risk events triggering continuous fan operation

Performance of the asynchronous zonal recirculation control (Phase II)

Phase II was initiated on 12 February 2026 and extended through 26 February 2026, covering a total monitoring interval of 15 days (360 hours). During this period, Vent1 (East compartment) continued to be driven by the canopy worst-case dew margin (S1), while Vent2 (West compartment) was independently controlled by the local canopy sensor S2, implementing the asynchronous zonal strategy described in the Materials and Methods section.

Over the 15-day interval, the recirculation system accumulated a total runtime of 63.1 hours, corresponding to a mean daily operation of 4.21 ± 2.30 h day^{-1}. The day-to-day variability in runtime was substantially higher than in Phase I (coefficient of variation: 55% vs. approximately 5% in the synchronized phase), reflecting the adaptive nature of the control logic responding to variable nocturnal conditions. On nights with more severe external conditions, daily runtimes reached up to 10.2 hours (21 February), while on milder nights the system operated as little as 2.3 hours, demonstrating the energy-modulating effect of the threshold-based hysteresis strategy.

The daily mean canopy dew margin for the eastern compartment (S1) ranged from 1.25°C to 10.45°C, with an overall mean of 5.24 ± 3.29°C. The western compartment (S2) exhibited slightly higher values, with a mean of 5.86 ± 3.49°C and a daily range of 1.34°C to 11.14°C. The persistent lateral asymmetry first identified during Phase I was maintained throughout Phase II, with S1 consistently recording lower daily mean dew margins than S2. This asymmetry is visually apparent in the

continuous monitoring record (Figure 3) and is consistent with the higher irrigation frequency in the eastern compartment noted in the Methods section.

The daily minimum dew margin - representing the closest approach to condensation within each 24-hour period - was maintained above 0.8°C for S1 (mean minimum: 1.10 ± 0.17°C, absolute minimum: 0.81°C on 25 February) and above 0.87°C for S2 (mean minimum: 1.24 ± 0.24°C). Critically, the cumulative condensation risk counter for the canopy zone recorded zero hours of active risk across all monitored days in Phase II, indicating that the dew margin remained above the 2°C intervention threshold for the dominant part of each day and that brief excursions below this threshold were successfully intercepted by recirculation activation.

A Spearman rank correlation analysis between daily recirculation runtime and daily minimum dew margin in the western compartment yielded a statistically significant negative association ($r_s = -0.582$, $p = 0.010$, $n = 15$), confirming that the control system responded appropriately to microclimatic pressure: higher recirculation effort was consistently associated with days of greater condensation proximity. A similar trend was observed for the eastern compartment ($r_s = -0.396$), though this did not reach statistical significance ($p = 0.12$), likely reflecting the more frequent activation of continuous-mode recirculation in S1 which partially saturated the runtime response.

The inter-phase comparison of daily mean dew margin values (Phase I: S1 mean 3.39 ± 1.80°C; Phase II: S1 mean 5.24 ± 3.29°C) indicates numerically higher margins in Phase II, consistent with generally milder external conditions during the later observation period (mean inter-layer temperature 3.60 ± 2.61°C in Phase II vs. 0.96 ± 3.50°C in Phase I). A Mann-Whitney U test did not identify a statistically significant difference between phases for either compartment (S1: $U = 58.0$, $z = -1.27$, $p = 0.20$; S2: $U = 65.0$, $z = -0.91$, $p = 0.36$), and the Spearman correlation between external temperature and daily dew margin did not reach significance in either phase (Phase II S1: $r_s = 0.34$, $p = 0.19$; Phase II S2: $r_s = 0.38$, $p = 0.14$). These results indicate that inter-phase differences in dew margin are not attributable to a single confounding thermal driver, though the relatively small sample sizes preclude definitive causal attribution.

Analysis of individual fan activation events confirmed the high degree of operational synchrony between the two ventilation units throughout Phase II, with Vent1 recording 90 total activations and Vent2 recording 83 activations over the 15-day period ($r = 0.856$, daily activation counts). Meaningful divergence between units was observed on only two days (17 and 18 February), when Vent1 activated three times more than Vent2, corresponding to the nights with the most pronounced S1-S2 dew margin asymmetry. These results indicate that, under the observed winter conditions, the microclimatic difference between the eastern and western compartments was insufficient to produce systematic operational decoupling of the two ventilation zones. The asynchronous zonal strategy nevertheless provided the control infrastructure for independent response, which may become more relevant under more contrasted lateral humidity conditions.

No leaf wetness events were detected at canopy level during Phase II, consistent with the results of Phase I and confirming the biological effectiveness of the control approach across both experimental configurations (Table 1, Table 2).

Late-phase lateral asymmetry (24 February - 3 March 2026)

Towards the end of Phase II, a progressive and sustained lateral asymmetry became evident between the eastern (S1) and western (S2) compartments (Figure 8). During the period 24 February - 3 March 2026, sensor S2 consistently recorded higher dew margin values than S1, with peak nocturnal differences exceeding 6°C. Both zones retained the characteristic diurnal pattern of low nocturnal margins and elevated daytime values driven by solar gain, yet the intensity of nocturnal condensation risk diverged substantially between compartments.

A probable contributing factor is differential irrigation between the two zones: higher water application in the eastern compartment would elevate local vapour pressure and reduce the dew margin independently of fan state, while the western zone - receiving less irrigation - maintained a consistently higher safety margin. This observation directly demonstrates the

agronomic value of asynchronous zonal control: Vent1, driven by S1, operated at higher activation frequency during this period, while Vent2, driven by S2, ran at reduced duty - delivering localised energy efficiency without compromising condensation prevention in the higher-risk eastern zone. This dynamic would be unachievable under the synchronised strategy of Phase I.

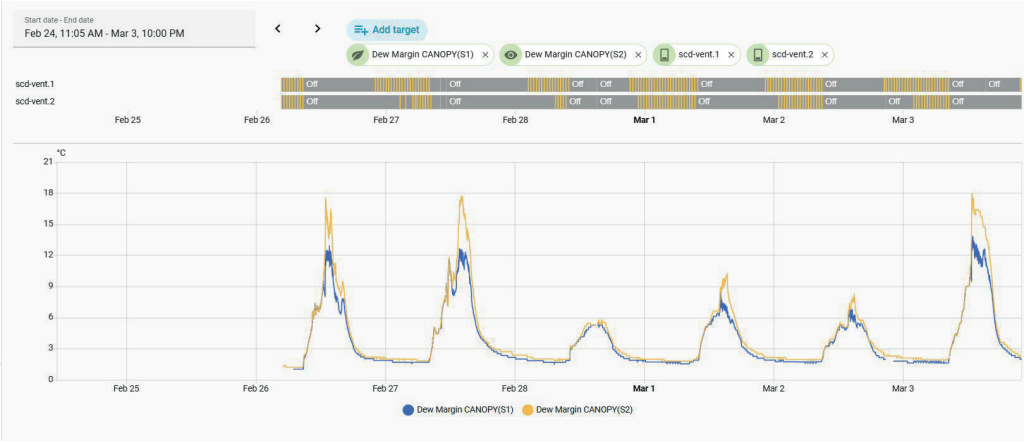


Figure 8. Canopy dew margin for S1 (East, blue) and S2 (West, yellow) during the final period of Phase II (24 February - 3 March 2026), with asynchronous ventilator activation states shown in the upper panel. A progressive lateral asymmetry is visible from 26 February onward, with S2 consistently exceeding S1 during nocturnal risk periods. The divergence is consistent with differential irrigation practices between compartments and illustrates the operational relevance of independent zonal control

Table 1. Summary statistics of canopy dew margin (ΔT, °C) for Sensor S1 (East, 170 cm) and Sensor S2 (West, 170 cm) during Phase I and Phase II

Parameter	Phase I S1 (East)	Phase I S2 (West)	Phase II S1 (East)	Phase II S2 (West)
Observation period (days)	11	11	15	15
Total monitoring hours (h)	264	264	360	360
Mean daily ΔT (°C)	3.39 ± 1.80	4.12 ± 2.43	5.24 ± 3.29	5.86 ± 3.49
Daily minimum ΔT – mean (°C)	–	–	1.10 ± 0.17	1.24 ± 0.24
Absolute minimum ΔT (°C)	0.55	1.41	0.81	0.87
5th percentile ΔT (°C)	1.57	1.93	0.89[1]	0.95[1]
Cumul. time below 2°C (h)	164.56 (62.3%)	139.11 (52.7%)	30.0 (8.3%)	20.3 (5.6%)
Cumul. time below 1°C (h)	0.09	0.00	~0.74[2]	–
Days with min ΔT < 1°C	–	–	5 / 15	2 / 15

Table 2. Recirculation fan operational statistics during Phase I and Phase II.

Parameter	Phase I	Phase II
Control strategy	Synchronized – both units driven by S1 worst-case	Asynchronous zonal – Vent1 by S1; Vent2 by S2
Observation period (days)	11	15
Total monitoring hours (h)	264	360
Cumulative runtime – Vent1 (h)	50.22	n.d.[1]
Cumulative runtime – Vent2 (h)	50.03	n.d.[1]
Mean daily runtime (h day^{-1})	4.56 ± 0.02[2]	4.21 ± 2.30

Parameter	Phase I	Phase II
Daily runtime range (h day^{-1})	4.55 – 4.57	2.25 – 10.22
Operational duty cycle (%)	19.0	17.5
Total activation events – Vent1	n.d.[1]	90
Total activation events – Vent2	n.d.[1]	83
Vent1 / Vent2 activation correlation	–[3]	r = 0.856

[1] n.d. = not directly available from database

[2] Near-zero standard deviation confirms fully deterministic synchronized operation in Phase I. [3] Synchronised operation in Phase I makes individual correlation analysis redundant — both units operated identically by design.

The results demonstrate that internal air recirculation, driven by canopy-level dew margin indicators, effectively prevented plant-level condensation throughout the monitoring period. The complete absence of leaf wetness events at canopy level - despite multiple nocturnal intervals of critical proximity - supports the central hypothesis that canopy-oriented control provides biologically relevant protection even when envelope condensation remains unavoidable. This distinction between structural and canopy condensation is consistent with Piscia et al. (2012) and Boulard et al. (2004), who showed that leaf boundary-layer humidity can differ substantially from bulk greenhouse air. The use of dew margin as a control variable proved essential in this context: RH values consistently exceeded 85–90% throughout the monitoring period, yet canopy condensation did not occur, illustrating the well-documented limitation of RH thresholds for site-specific condensation risk assessment (Wang et al., 2019).

The persistent lateral S1-S2 asymmetry, observed in both phases, is consistent with the broader literature emphasising that spatial heterogeneity may persist even in actively mixed greenhouses, and that stagnant zones can remain localised condensation hotspots independent of bulk conditions (Bournet and Boulard, 2010; Gao et al., 2024). Although Phase II produced high operational synchrony between ventilation units (r = 0.856), this reflects the relatively moderate lateral contrast observed during the specific monitoring period rather than a failure of the zonal architecture. The asynchronous configuration provides the control infrastructure for independent zonal response, which may become operationally decisive under more contrasted humidity conditions - for instance, following differential irrigation events or under asymmetric solar radiation patterns.

From an energy perspective, the recirculation system operated at duty cycles of 19.0% (Phase I) and 17.5% (Phase II), corresponding to a mean daily energy consumption of approximately 3.6-3.7 kWh for recirculation alone - a modest fraction of the thermal energy that would have been required for equivalent dehumidification through external ventilation under the same conditions (Maslak & Nimmermark, 2017; Amani et al., 2020). The adaptive three-regime control strategy ensured that fan operation was restricted to periods of genuine microclimatic need, contributing to the relatively low overall duty cycle.

Several limitations must be acknowledged. The absence of a concurrent unventilated control treatment prevents direct causal attribution of condensation prevention to the recirculation system, and the inter-phase comparison was confounded by differences in external thermal conditions between the two monitoring periods. The Mann-Whitney comparison between phases did not reach statistical significance ($p > 0.20$), meaning that the observed numerical differences in dew margin cannot be unambiguously attributed to the change in control strategy rather than to more favourable meteorological conditions. Air velocity measurements were also limited to two positions and a single session, precluding full characterisation of the three-dimensional airflow field. Despite these limitations, the study contributes a reproducible, low-cost methodology for preventive condensation-risk management based on distributed dew point monitoring and threshold-driven recirculation, integrated within a unified Home Assistant and InfluxDB infrastructure replicable without specialised instrumentation.

CONCLUSIONS

Internal air recirculation driven by canopy dew margin indicators successfully prevented plant-level condensation in a passive double-layer solar greenhouse throughout the winter monitoring period, with zero leaf wetness events recorded at canopy level despite persistent nocturnal condensation on structural surfaces.

The dew margin indicator proved more operationally discriminating than relative humidity alone for condensation risk control, enabling the system to maintain biologically safe canopy conditions even when bulk RH consistently exceeded 85-90%.

A persistent lateral microclimate asymmetry between the eastern and western compartments was identified in both experimental phases, providing experimental justification for the asynchronous zonal control architecture, even though operational decoupling between ventilation units remained limited under the observed meteorological conditions.

The recirculation system operated at duty cycles of 17-19% of total monitoring time, with mean daily runtimes of 4.2-4.6 h day^{-1}, confirming that the energy cost of internal mixing is modest compared to equivalent dehumidification through external ventilation.

The integrated monitoring and control framework - combining distributed dew point sensing, adaptive threshold-based automation, and continuous time-series archiving - represents a reproducible methodology applicable to other passive greenhouse contexts without specialised instrumentation.

ACKNOWLEDGEMENTS

The author acknowledges the technical infrastructure provided by the University of Agronomic Sciences and Veterinary Medicine of Bucharest and the support of the Home Assistant open-source community for automation tools used in data acquisition and control.

REFERENCES

Amani, M., Foroushani, S., Sultan, M., & Bahrami, M. (2020). Comprehensive review on dehumidification strategies for agricultural greenhouse applications. *Applied Thermal Engineering, 181*, 115979.

Baptista, F. J., Bailey, B. J., Randall, J. M., & Meneses, J. F. (1999). Greenhouse ventilation rate: Theory and measurement with tracer gas techniques. *Journal of Agricultural Engineering Research, 72,* 363–374.

Blanchard, M. (2008). Fanning uniformity in the greenhouse. Greenhouse Product News, May 2008, 66.

Boulard, T., & Draoui, B. (1995). Natural ventilation of a greenhouse with continuous roof vents: Measurements and data analysis. *Journal of Agricultural Engineering Research, 61*, 27–36.

Boulard, T., Fatnassi, H., Roy, J. C., Lagier, J., Fargues, J., Smits, N., Rougier, M., & Jeannequin, B. (2004). Effect of greenhouse ventilation on humidity of inside air and in leaf boundary-layer. *Agricultural and Forest Meteorology, 125,* 225–239. https://doi.org/10.1016/j.agrformet.2004.04.005

Bournet, P.-E., & Boulard, T. (2010). Effect of ventilator configuration on the distributed climate of greenhouses: A review of experimental and CFD studies. *Computers and Electronics in Agriculture, 74,* 195–217. https://doi.org/10.1016/j.compag.2010.08.007

Gao, Z., Li, W., Li, W., & Ding, X. (2024). Experimental research on the microclimate in the naturally ventilated multi-span greenhouse. *International Journal of Agricultural and Biological Engineering, 17(3)*, 68–74. https://doi.org/10.25165/j.ijabe.20241703.7073

He, K.-S., Chen, D.-Y., Sun, L.-J., Liu, Z.-L., & Huang, Z.-Y. (2015). The effect of vent openings on the microclimate inside multi-span greenhouses during summer and winter seasons. *Engineering Applications of Computational Fluid Mechanics, 9*(1), 399–410.

Katsoulas, N., Bartzanas, T., Boulard, T., Mermier, M., & Kittas, C. (2006). Effect of vent openings and insect screens on greenhouse ventilation. *Biosystems Engineering, 93*(4), 427–436.

Kittas, C., Karamanis, M., & Katsoulas, N. (2005). Air temperature regime in a forced ventilated greenhouse with rose crop. *Energy and Buildings, 37*, 807–812.

Lee, T., Kang, G., Jang, J., Paek, Y., & Lim, R. (2020). Analysis on the effect of greenhouse humidity control by counter-flow ventilator in winter. *Protected Horticulture and Plant Factory, 29*(3), 259–264.

Maslak, K., & Nimmermark, S. (2017). Thermal energy use for dehumidification of a tomato greenhouse by natural ventilation and a system with an air-to-air heat exchanger. *Agricultural and Food Science, 26,* 56–66.

Piscia, D., Montero, J. I., Baeza, E., & Bailey, B. J. (2012). A CFD greenhouse night-time condensation model. *Biosystems Engineering, 111*, 141–154. https://doi.org/10.1016/j.biosystemseng.2011.11.006

Sase, S., Kozai, T., Nara, M., & Negishi, H. (1980). Ventilation of greenhouses. I. Wind tunnel measurements of pressure and discharge coefficients for a single-span greenhouse. *Journal of Agricultural Meteorology, 36(1)*, 3–12.

Sase, S. (2006). Air movement and climate uniformity in ventilated greenhouses. In B. J. Bailey (Ed.), *Proceedings of the International Symposium on*

Greenhouse Cooling. Acta Horticulturae, 719, 313–324.

Teitel, M., & Tanny, J. (1999). Natural ventilation of greenhouses: Experiments and model. *Agricultural and Forest Meteorology, 96*, 59–70.

Tusi, A., & Shimazu, T. (2020). The essential factor of ventilation rate in prediction of photosynthetic rate using the CO_2 balance method. Reviews in Agricultural Science, 8, 279–299. https://doi.org/10.7831/ras.8.0_279

Wang, H., Sánchez-Molina, J. A., Li, M., & Rodríguez Díaz, F. (2019). Improving the performance of vegetable leaf wetness duration models in greenhouses using decision tree learning. *Water, 11*, 158. https://doi.org/10.3390/w11010158.

Wang, Z., Bao, A., Li, J., He, J., Wang, K., Wang, X., & Sun, X. (2025). Study on the effect of non-uniform ventilation on energy and plant growth in a greenhouse. *Horticulturae, 11*(2), 166. https://doi.org/10.3390/horticulturae11020166

Zhang, Y., Sun, W., Jin, L., Yang, H., Wang, J., & Shu, S. (2025). Computational fluid dynamics-based simulation of ventilation in a zigzag plastic greenhouse. *Horticulturae, 11*(2), 175. https://doi.org/10.3390/horticulturae11020.